

The connection between metallicity and metal-line kinematics in (sub-)damped Lyman- α systems

M. T. Murphy^{1*}, S. J. Curran², J. K. Webb², H. Ménager^{1,2}, B. J. Zych¹

¹*Institute of Astronomy, University of Cambridge, Madingley Road, Cambridge CB3 0HA*

²*School of Physics, University of New South Wales, Sydney NSW 2052, Australia*

Accepted 2006 December 29. Received 2006 December 29; in original form 2006 October 27

ABSTRACT

A correlation between the metallicity, $[M/H]$, and rest-frame Mg II equivalent width, $W_r^{\lambda 2796}$, is found from 49 DLAs and strong sub-DLAs drawn from the literature over the redshift range $0.2 < z_{\text{abs}} < 2.6$. The correlation is significant at 4.2σ and improves to 4.7σ when the mild evolution of $[M/H]$ with redshift is taken into account. Even when including only the 26 DLAs (i.e. excluding sub-DLAs) which have Zn-metallicities and $W_r^{\lambda 2796} > 0.7 \text{ \AA}$, the correlation remains at $> 3\sigma$ significance. Since the Mg II $\lambda 2796$ transition is predominantly saturated in DLAs (which always have $W_r^{\lambda 2796}$ greater than 0.3 \AA), $W_r^{\lambda 2796}$ is far more sensitive to the kinematic spread of the metal velocity components across the absorption profile than it is to $[M/H]$. Thus, the observed $[M/H]$ – $W_r^{\lambda 2796}$ correlation points to a strong link between the absorber metallicity and the mechanism for producing and dispersing the velocity components. We also note that approximately half of the 13 known H₂ absorbers have very high $W_r^{\lambda 2796}$ and very broad velocity structures which show characteristics usually associated with outflows. Follow-up ultraviolet- and blue-sensitive high-resolution spectra of high- $W_r^{\lambda 2796}$ systems, initially identified in low-resolution spectra, may therefore yield a large number of new H₂ discoveries.

Key words: intergalactic medium – quasars: absorption lines – cosmology: observations – galaxies: evolution – galaxies: ISM

1 INTRODUCTION

The damped Lyman- α absorbers (DLAs) observed along sight-lines to quasars (QSOs) are potentially important pieces in the puzzle of galaxy formation. They are the highest column density absorption systems, with $N(\text{H I}) \geq 2 \times 10^{20} \text{ cm}^{-2}$, and the first DLA surveys quickly established that they contain a large fraction of the high- z baryons *available* for star formation (Wolfe et al. 1986; Lanzetta et al. 1991). The early estimates of the neutral gas mass density at absorption redshifts $z_{\text{abs}} \sim 3$ were similar to the estimates of the mass density in stars at $z = 0$. It was therefore natural to assume that DLAs act as the neutral gas reservoirs for star formation. However, firmly establishing the link between DLAs and star formation relies on our understanding of the absorber–galaxy connection. Direct imaging of DLAs (or strong Mg II systems; see below) at $z_{\text{abs}} < 1.5$ reveals the hosts to be a mix of irregulars, dwarfs, spirals and low surface-brightness galaxies (e.g. Bergeron & Boissé 1991; Le Brun et al. 1997; Rao et al. 2003; Chen & Lanzetta 2003). This is further borne out by a blind 21-cm emission survey at $z = 0$ (Ryan-Weber et al. 2003). However, quantifying the mix of DLA host-galaxy morphologies from low- to high-redshift is fraught with selection effects, not least

of which are luminosity bias against faint galaxies and the proximity of some host-galaxies to the QSO sight-line. Indeed, very few DLA host-galaxies have been identified at $z_{\text{abs}} \geq 2$ (e.g. Møller & Warren 1993; Djorgovski et al. 1996; Christensen et al. 2005; Weatherley et al. 2005).

The Mg II $\lambda 2796/2803$ doublet has proved very important for exploring the absorber–galaxy connection at $0.3 \lesssim z_{\text{abs}} \lesssim 2.6$ where it is observable with optical QSO absorption spectroscopy. Indeed, many of the $z_{\text{abs}} < 1.5$ imaging studies above initially identified absorption systems via the easily recognised Mg II doublet (see also, e.g., Lanzetta & Bowen 1990; Bergeron et al. 1992; Steidel & Sargent 1992; Drinkwater et al. 1993; Steidel et al. 1994). Also, since the ionization potential of Mg I is $< 13.6 \text{ eV}$ but that of Mg II is $> 13.6 \text{ eV}$, the latter traces cold gas. Attempts have therefore been made to identify DLA candidates at low- z_{abs} via their Mg II absorption (e.g. Rao et al. 1995, 2006; Ellison 2006). The Mg II doublet transitions are also among the strongest metal lines observed in QSO absorbers, meaning that (i) the Mg II $\lambda 2796$ rest-frame equivalent width in DLAs is typically $W_r^{\lambda 2796} \geq 0.3 \text{ \AA}$, allowing such systems to be identified in relatively low-resolution spectra, and (ii) most velocity components across the Mg II profile are saturated in DLAs. This implies that $W_r^{\lambda 2796}$ is mainly sensitive to the kinematic extent of the velocity components, Δv , rather than

* E-mail: mim@ast.cam.ac.uk

their column density. A good demonstration of this is figure 3 of Ellison (2006).

In this paper we search for a relationship between $W_r^{\lambda 2796}$ and the metallicity¹, $[M/H]$, of DLAs and strong sub-DLAs. Since $W_r^{\lambda 2796}$ is a measure of the kinematic spread of the cold, metal-bearing velocity components, such a relationship may constrain the mechanisms for producing and dispersing the metals. This may guide our understanding of the physical nature of DLAs.

There currently exist only indirect and possibly contradictory constraints on a $[M/H]$ - $W_r^{\lambda 2796}$ relationship for DLAs and sub-DLAs. Nestor et al. (2003) suggest that $[M/H]$ increases with increasing $W_r^{\lambda 2796}$. They identified strong Mg II systems in Sloan Digital Sky Survey (SDSS) QSO spectra over the redshift range $0.9 < z_{\text{abs}} < 2.0$ and constructed composite spectra in the absorber rest-frame. The Zn II lines were stronger in the composite of $W_r^{\lambda 2796} \geq 1.3 \text{ \AA}$ absorbers compared with those in the composite of $1.0 < W_r^{\lambda 2796} < 1.3 \text{ \AA}$ systems. Assuming that the mean $N(\text{H I})$ is not significantly different in these two regimes, they conclude that some evidence exists for a $[\text{Zn}/\text{H}]$ - $W_r^{\lambda 2796}$ correlation. On the other hand, York et al. (2006) find less direct evidence for an anti-correlation between $[\text{Zn}/\text{H}]$ and $W_r^{\lambda 2796}$. From a series of composite SDSS spectra with various mean $W_r^{\lambda 2796}$ they find that the dust-reddening, $E(B - V)$, caused by the absorbers rises sharply with increasing $W_r^{\lambda 2796}$. While the Zn II line-strengths also increase, they show a slower increase than $E(B - V)$ over the same range of $W_r^{\lambda 2796}$. The composite spectra also suggest a dust extinction curve typical of the Small Magellanic Cloud (SMC), leading York et al. to assume a constant dust-to-gas ratio, i.e. $N(\text{H I}) \propto E(B - V)$, as observed in the SMC. Thus, since the Zn II column density increases slower than the $N(\text{H I})$ inferred from $E(B - V)$ under this assumption, York et al. (2006) argue that $[\text{Zn}/\text{H}]$ decreases with increasing $W_r^{\lambda 2796}$. We discuss these results further in light of our new results in Section 3.

This paper is organised as follows. Section 2 explains our sample selection and explores an evident $[M/H]$ - $W_r^{\lambda 2796}$ relationship in that sample. Section 3 compares our results with the $[M/H]$ - Δv correlation recently discovered by Ledoux et al. (2006) at (generally) higher redshifts. We also discuss whether our observed $[M/H]$ - $W_r^{\lambda 2796}$ relationship can be taken as evidence for a correlation or anti-correlation between absorber metallicity and host-galaxy mass. Finally, we discuss whether a large fraction of strong Mg II absorbers might arise in outflows from relatively low mass galaxies. In particular, about half of those absorbers in which H₂ has been detected show some evidence of an outflow origin.

2 CORRELATION BETWEEN METALLICITY AND MG II EQUIVALENT WIDTH IN DLAS AND SUB-DLAs

2.1 Sample definition

We identified DLAs [$N(\text{H I}) \geq 2 \times 10^{20} \text{ cm}^{-2}$] and strong sub-DLAs [$N(\text{H I}) \geq 3 \times 10^{19} \text{ cm}^{-2}$] with existing metallicity measurements in the compilation of Kulkarni et al. (2005) and several other, typically more recent, sources (as cited in Table 1). For these systems we searched the literature for $W_r^{\lambda 2796}$ measurements; Table 1 lists those systems for which we found both $[M/H]$ and $W_r^{\lambda 2796}$. Uncertainties for some $W_r^{\lambda 2796}$ values could not be found in the lit-

erature (see Section 2.2). For systems without a published $W_r^{\lambda 2796}$ value we searched for publicly available SDSS ($R \sim 2000$) or Very Large Telescope Ultraviolet and Visual Echelle Spectrograph (VLT/UVES; $R \geq 40000$) spectra from which an $W_r^{\lambda 2796}$ measurement is easily made. For SDSS spectra, our method for obtaining $W_r^{\lambda 2796}$ is described in detail in Bouché et al. (2006). UVES spectra were obtained from the ESO data archive and reduced using a version of the UVES pipeline which we modified to improve the flux extraction and wavelength calibration. The extracted echelle orders from all exposures were combined, using UVES POPLER², with inverse-variance weighting and a cosmic ray rejection algorithm, to form a single spectrum with a dispersion of $2.5 \text{ km s}^{-1} \text{ pixel}^{-1}$. $W_r^{\lambda 2796}$ was then measured by direct summation of pixels across the Mg II $\lambda 2796$ profile. The uncertainties in $W_r^{\lambda 2796}$ quoted in Table 1 for these UVES spectra are generally dominated by uncertainties in the continuum level around the Mg II $\lambda 2796$ line. In some cases where $W_r^{\lambda 2796}$ is so high that the $\lambda 2796$ profile is blended with that of the $\lambda 2803$ line (typically $W_r^{\lambda 2796} \geq 3.5 \text{ \AA}$), larger uncertainties are reported.

For most of the 49 absorbers in Table 1, Zn-metallicities were available in the literature. In 13 cases we have used the Fe or Cr abundance in the absence of a Zn measurement. It is well known that these elements are depleted onto dust grains (e.g. Pettini et al. 1997) and so we corrected the Fe and Cr abundances with the simple prescription of Prochaska et al. (2003a): $[M/H] = [\text{Fe}/\text{H}] + 0.4 = [\text{Cr}/\text{H}] + 0.2$. In Section 2.2 we test the possible impact this might have on our results. Most of the metallicities in Table 1 have been corrected to the solar scale of Lodders (2003). The values quoted in the literature were used for Q 0235+164, Q 1622+238, Q 0458-020, Q 1122-1649, Q 1157+014 since we could not identify which solar values the original authors used. Since the corrections are typically $\lesssim 0.1$ dex, these 5 exceptions have negligible impact on our main results.

2.2 The $W_r^{\lambda 2796}$ - $[M/H]$ correlation

Figure 1(left) shows all the $[M/H]$ - $W_r^{\lambda 2796}$ pairs. Table 1 gives the formal statistical errors on both quantities as reported in the literature. In cases where no error-bars could be found in the literature, uncertainties of 0.10 dex and 0.05 \AA were assumed as these typified the rest of the sample. For Fig. 1(left) we added 0.05 dex and 0.03 \AA in quadrature to the initial $[M/H]$ and $W_r^{\lambda 2796}$ uncertainties to take into account likely continuum fitting errors which are not included by some authors or, indeed, by our own $W_r^{\lambda 2796}$ measurements in SDSS spectra. We regard the points in Table 1 with these increased errors as our fiducial sample. Kendall's τ for the $[M/H]$ - $W_r^{\lambda 2796}$ correlation evident in Fig. 1 has a probability $P(\tau) = 2.6 \times 10^{-5}$ of being due to chance alone; assuming Gaussian statistics, the correlation is significant at $> 4.2\text{-}\sigma$. The correlation is robust to the removal of distinct sub-samples, some of which are discussed below, as shown in Table 2.

The absorbers cover quite a large redshift range, $0.2 < z_{\text{abs}} < 2.6$, so evolution in DLA metallicities may have somewhat washed out the correlation we observe. For example, if absorbers at lower z_{abs} are, on average, more metal-rich than at higher z_{abs} , then this would cause additional dispersion in $[M/H]$ at all values of $W_r^{\lambda 2796}$. This would at least decrease the statistical significance of the observed correlation and, depending on the redshift distribution of the

¹ Metallicity is defined as the heavy element abundance with respect to hydrogen, relative to that of the solar neighbourhood: $[M/H] \equiv \log[N(\text{M})/N(\text{H})] - \log[N(\text{M})/N(\text{H})]_{\odot}$

² Available at http://www.ast.cam.ac.uk/~mim/UVES_popler.html

Table 1. DLAs and sub-DLAs where both Mg II $\lambda 2796$ Å equivalent width, W_r^{2796} , and metallicity, [M/H], have been measured. B1950 QSO names are given. $N(\text{H I})$ is the total neutral hydrogen column density [cm^{-2}], z_{abs} is the DLA redshift and z_{em} is the redshift of the background QSO. Errors on W_r^{2796} and [M/H] are quoted from the literature but in many cases do not include continuum-fitting uncertainties. [M/H] is measured relative to the solar abundances of Lodders (2003) in most cases (see text). The element used to determine [M/H] is Zn where possible; when this is not available we corrected for dust depletion via $[\text{M}/\text{H}] = [\text{Fe}/\text{H}] + 0.4 = [\text{Cr}/\text{H}] + 0.2$ (see Prochaska et al. 2003a).

QSO	$\log N(\text{H I})$	z_{abs}	z_{em}	W_r^{2796} [Å]	Ref.	[M/H]	M	Ref.	Notes
0013–0029	20.8	1.973	2.08694	4.7 ± 0.3	R03	-0.72 ± 0.09	Zn	P02	<i>a</i>
0058+0155	20.1	0.61251	1.954	1.68 ± 0.03	HIRES	$+0.05 \pm 0.21$	Zn	P00	—
0100+130	21.4	2.3091	2.681	0.85 ± 0.01	UVES ^{7,19}	-1.54 ± 0.09	Zn	PW99	PHL 957
0235+164	21.7	0.52385	0.94	2.34 ± 0.05	LB92	-0.22 ± 0.15	Zn	J04,P03a	<i>b</i>
0302–223	20.4	1.00945	1.409	1.16 ± 0.04	R06	-0.56 ± 0.12	Zn	P00	<i>e</i>
0405–4418	21.0	2.5505	3.00	2.38 ± 0.25	UVES ^{10,11,14}	-1.32 ± 0.11	Zn	LE03	CTQ 0247
0405–4418	21.1	2.595	3.00	1.29 ± 0.09	UVES ^{10,11,14}	-1.04 ± 0.10	Zn	LE03	<i>a</i> , CTQ 0247
0454+039	20.7	0.8596	1.345	1.45 ± 0.01	C00	-0.99 ± 0.12	Zn	P00	<i>c</i>
0458–020	21.7	2.03945	2.286	1.69 ± 0.07	W93	-1.19 ± 0.09	Zn	PW99	<i>b</i>
0512–3329	20.5	0.931	1.569	1.94	E06b	-1.09 ± 0.11	Fe	L05	—
0515–4414	20.5	1.1508	1.713	2.34 ± 0.02	UVES ^{1,5,16}	-0.95 ± 0.19	Zn	D00	<i>a</i>
0528–250	20.6	2.141	2.813	1.89 ± 0.08	UVES ^{6,9,11}	-1.45 ± 0.07	Zn	C03a	<i>d</i>
0551–366	20.4	1.962	2.318	5.80 ± 0.08	R03	-0.11 ± 0.09	Zn	L02b	<i>a</i>
0738+313	20.8	0.2212	0.635	0.61 ± 0.04	B87	-1.24 ± 0.2	Cr	K04	<i>b</i>
0827+243	20.3	0.5247	0.939	2.90	RT00	-0.62 ± 0.08	Fe	K04	<i>b</i>
0841+1256	21.3	2.3745	2.50	0.76 ± 0.07	UVES ^{2,15}	-1.47 ± 0.15	Zn	PW99	—
0933+732	21.6	1.4789	2.528	0.95 ± 0.08	R06	-1.58 ± 0.25	Zn	K04	<i>e</i>
0935+417	20.3	1.3726	1.98	1.04	P04	-0.78 ± 0.2	Zn	M95	—
0945+436	21.5	1.223	1.89149	1.12 ± 0.05	SDSS	-0.95 ± 0.10	Zn	P03a	—
0949+527	20.1	1.7678	1.87476	3.88 ± 0.05	SDSS	$+0.02 \pm 0.10$	Zn	P06b	—
0952+179	21.3	0.2378	1.472	0.63 ± 0.11	RT00	-1.45 ± 0.2	Cr	K05	<i>b</i>
0957+561A	20.3	1.391	1.413	2.25	E06b	-0.91	Fe	C03b	<i>c</i>
0957+561B	19.9	1.391	1.413	2.13	E06b	-0.63	Fe	C03b	<i>c</i>
1101–264	19.5	1.838	2.145	0.94	E06b	-1.06 ± 0.07	Fe	D03	—
1104–1805	20.9	1.6614	2.319	0.96	L99	-0.99 ± 0.02	Zn	L99	—
1104+0104	21.0	0.7404	1.3924	2.95 ± 0.03	R06	-0.60 ± 0.2	Zn	K04	—
1122–1649	20.5	0.6819	2.40	1.72	P04	-1.00 ± 0.15	Fe	L02a,P03a	<i>d</i>
1151+068	21.3	1.7736	2.762	0.52 ± 0.05	R03	-1.53 ± 0.14	Zn	P97	—
1157+014	21.8	1.94362	1.986	1.38 ± 0.06	R03	-1.36 ± 0.12	Zn	L03	<i>b</i>
1209+093	21.4	2.5840	3.297	3.20 ± 0.50	UVES ^{8,18}	-1.04 ± 0.11	Zn	P03b	<i>e</i>
1210+1731	20.6	1.892	2.543	1.09	E06b	-0.86 ± 0.10	Zn	D06	—
1215+333	21.0	1.999	2.606	1.03 ± 0.15	SS92	-1.25 ± 0.09	Zn	P99	<i>d</i>
1223+1753	21.5	2.4658	2.936	1.54 ± 0.06	UVES ^{3,4,13}	-1.58 ± 0.10	Fe	P01	<i>e</i>
1229–0207	20.8	0.39498	1.045	2.17 ± 0.07	LB92	-0.45 ± 0.19	Zn	B98	<i>b</i>
1247+267	19.9	1.22319	2.038	0.42	E06b	-1.02 ± 0.25	Zn	P99	<i>d</i>
1320–0006	20.2	0.716	1.38839	2.13 ± 0.05	SDSS	$+0.61 \pm 0.20$	Zn	P06a	—
1328+307	21.3	0.692154	0.849	0.33	SM79	-1.20	Zn	MY92	<i>b</i> , 3C 286
1331+170	21.2	1.77642	2.084	1.33 ± 0.09	R03	-1.26 ± 0.10	Fe	P01	<i>a</i> , <i>b</i>
1351+318	20.2	1.14913	1.326	1.25	E06b	-0.27 ± 0.17	Zn	P99	<i>d</i>
1354+258	21.5	1.4205	2.006	0.61	RT00	-1.58 ± 0.16	Zn	K05	<i>c</i>
1451+123	19.9	2.255	3.246	1.20 ± 0.08	UVES ²	-1.08 ± 0.23	Zn	D05	<i>e</i>
1622+238	20.4	0.6561	0.927	1.29	SS92	-0.87 ± 0.25	Fe	P03a	<i>d</i> , 3C 336
1629+120	19.7	0.9008	1.795	1.20 ± 0.09	R06	-0.18	Zn	E06a	<i>d</i>
1727+5302	21.2	0.9448	1.444	2.832 ± 0.070	R06	-0.52 ± 0.2	Zn	K04	—
1727+5302	21.4	1.0312	1.444	0.922 ± 0.057	R06	-1.39 ± 0.2	Zn	K04	—
2206–1958	20.5	1.9205	2.56	1.99 ± 0.05	UVES ^{3,17,19}	-0.37 ± 0.07	Fe	P01	—
2231–0015	20.5	2.066	3.015	1.80	E06b	-0.86 ± 0.10	Zn	D04	<i>e</i>
2343+125	20.3	2.4310	2.549	3.22 ± 0.15	UVES ^{6,12,17}	-0.74 ± 0.08	Zn	D04	<i>a</i> , <i>e</i>
2348–1444	20.6	2.279	2.94	0.32	E06b	-1.84	Fe	D06	<i>d</i>

Notes: ^aH₂ absorption detected; ^b21-cm absorption detected; ^c21-cm absorption not detected; ^dradio-loud but not searched for 21-cm absorption; ^eradio-quiet. ¹60.A-9022 UVES commissioning; ²65.O-0063 Ledoux; ³65.O-0158 Pettini; ⁴65.P-0038 Srianand; ⁵66.A-0212 Reimers; ⁶66.A-0594 Molaro; ⁷67.A-0022 D’Odorico; ⁸67.A-0146 Vladilo; ⁹68.A-0106 Petitjean; ¹⁰68.A-0361 Lopez; ¹¹68.A-0600 Ledoux; ¹²69.A-0204 D’Odorico; ¹³69.B-0108 Srianand; ¹⁴70.A-0017 Petitjean; ¹⁵70.B-0258 Dessauges-Zavadsky; ¹⁶072.A-0100 Murphy; ¹⁷072.A-0346 Ledoux; ¹⁸073.B-0787 Dessauges-Zavadsky; ¹⁹074.A-0201 Srianand.

References: SM79 (Spinrad & McKee 1979), B87 (Boulade et al. 1987), W93 (Wolfe et al. 1985), LB92 (Lanzetta & Bowen 1992), MY92 (Meyer & York 1992), SS92 (Steidel & Sargent 1992), A94 (Aldcroft et al. 1994), M95 (Meyer et al. 1995), P97 (Pettini et al. 1997), B98 (Boisse et al. 1998), L99 (Lopez et al. 1999), P99 (Pettini et al. 1999), PW99 (Prochaska & Wolfe 1999), C00 (Churchill et al. 2000), D00 (de la Vega et al. 2000), P00 (Pettini et al. 2000), RT00 (Rao & Turnshek 2000), P01 (Prochaska et al. 2001), P02 (Petitjean et al. 2002), L02a (Ledoux et al. 2002), L02b (Ledoux et al. 2002), C03a (Centurión et al. 2003), C03b (Churchill et al. 2003), D03 (Dessauges-Zavadsky et al. 2003), L03 (Ledoux et al. 2003), LE03 (Lopez & Ellison 2003), P03a (Prochaska et al. 2003a), P03b (Prochaska et al. 2003b), R03 (Ryabinkov et al. 2003) [and references therein], D04 (Dessauges-Zavadsky et al. 2004), J04 (Junkkarinen et al. 2004), K04 (Khare et al. 2004), P04 (Péroux et al. 2004), A05 (Akerman et al. 2005), K05 (Kulkarni et al. 2005), L05 (Lopez et al. 2005), D06 (Dessauges-Zavadsky et al. 2006), E06a (Ellison 2006), E06b (S. E. Ellison, private communication), P06a (Péroux et al. 2006), P06b (Prochaska et al. 2006), R06 (Rao et al. 2006). ‘SDSS’ or ‘UVES’ indicates we have obtained W_r^{2796} from Sloan Digital Sky Survey spectra or from VLT/UVES spectra.

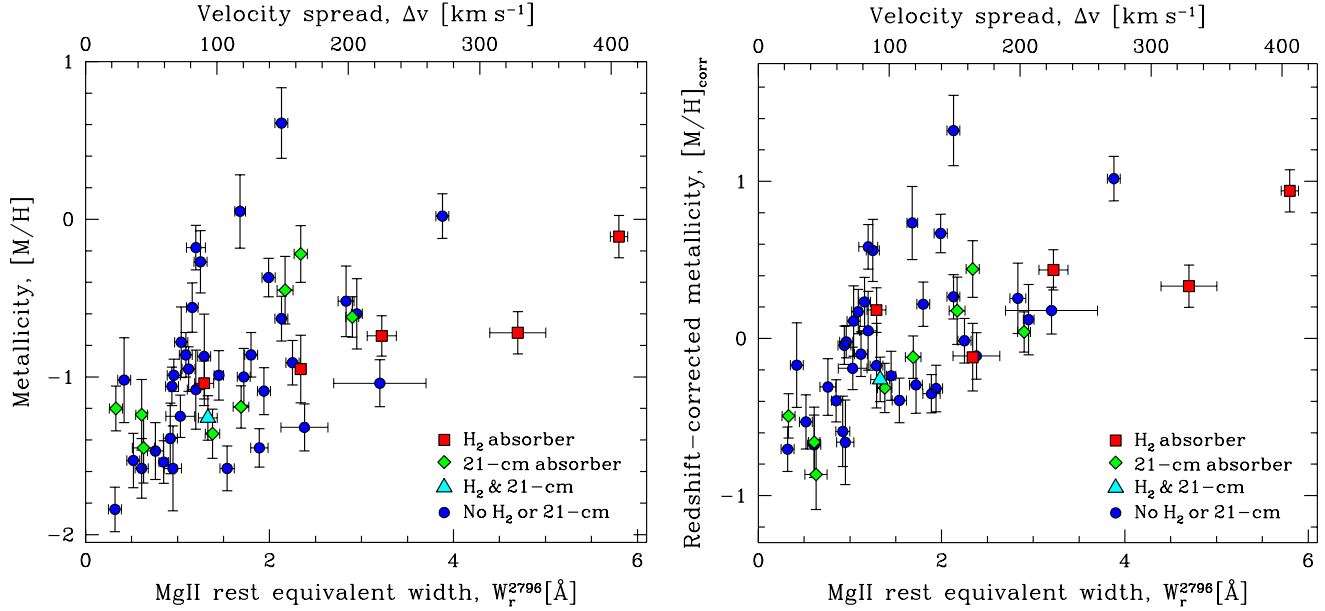


Figure 1. Correlation between absorber metallicity, $[M/H]$, and $Mg\ II$ rest-frame equivalent width, W_r^{12796} . The upper velocity scale is the approximate velocity spread calculated simply from $\Delta v [\text{km s}^{-1}] \approx 70 [\text{km s}^{-1} \text{ \AA}^{-1}] \times W_r^{12796} [\text{ \AA}]$. *Left:* Original data from Table 1 with additional $[M/H]$ - and W_r^{12796} -uncertainties of 0.05 dex and 0.03 \AA added in quadrature (see text). The correlation is significant at the 4.2σ level. *Right:* The $[M/H]$ values have been corrected for cosmological metallicity evolution according to equation (1). This reduces the scatter, improving the correlation to the 4.7σ level.

Table 2. Statistics for different sub-samples. N_a is the sample size. $\langle W_r^{12796} \rangle$ and $\langle [M/H] \rangle$ are the median rest-frame $Mg\ II$ equivalent width and the median metallicity, respectively. Columns 5–8 show the correlation statistics for the original data from Table 1 (with increased errors) while columns 9–12 show the same statistics after the metallicities are corrected for redshift evolution (see text). $P(\tau)$ is Kendall’s τ two-sided probability that no correlation exists between $[M/H]$ and W_r^{12796} . We convert this to a significance, $S(\tau)$, assuming Gaussian statistics. In all cases a Spearman test gives a more significant correlation. A and B are the intercept and slope, respectively, of the fit to the $[M/H]$ versus Δv data (see Section 3.1).

Sample	N_a	$\langle W_r^{12796} \rangle$ [\AA]	$\langle [M/H] \rangle$ [dex]	$P(\tau)$ [10^{-3}]	$S(\tau)$ [σ]	Original data		Redshift-corrected metallicities			
						A [dex]	B [dex]	$P(\tau)$ [10^{-3}]	$S(\tau)$ [σ]	A [dex]	B [dex]
0: Fiducial	49	1.38	-0.99	0.026	4.2	-4.29 ± 0.38	1.69 ± 0.20	0.0032	4.7	-3.24 ± 0.35	1.62 ± 0.18
1: $[Zn/H]$ only	36	1.33	-0.97	0.48	3.5	-4.28 ± 0.46	1.70 ± 0.24	0.038	4.1	-3.14 ± 0.40	1.60 ± 0.21
2: DLAs only	40	1.42	-1.02	0.028	4.2	-3.85 ± 0.28	1.41 ± 0.14	0.0011	4.9	-2.86 ± 0.28	1.38 ± 0.14
3: $W_r^{12796} > 0.7 \text{ \AA}$	42	1.69	-0.93	2.3	3.1	-4.96 ± 0.50	1.99 ± 0.25	1.7	3.1	-3.70 ± 0.44	1.83 ± 0.22
4: $1 + 2 + 3$	26	1.57	-0.97	2.2	3.1	-4.25 ± 0.35	1.59 ± 0.17	0.35	3.6	-2.97 ± 0.34	1.44 ± 0.16
5: $W_r^{12796} < 1.4 \text{ \AA}$	25	0.96	-1.20	9.7	2.6	-4.54 ± 0.70	1.91 ± 0.39	1.8	3.1	-3.67 ± 0.63	1.94 ± 0.35
6: $W_r^{12796} > 1.4 \text{ \AA}$	24	2.21	-0.73	100	1.6	-5.88 ± 1.32	2.33 ± 0.58	17	2.4	-5.33 ± 0.88	2.50 ± 0.39
7: $z_{\text{abs}} < 1.4$	24	1.56	-0.82	20	2.3	-3.98 ± 0.57	1.64 ± 0.30	46	2.0	-3.28 ± 0.60	1.67 ± 0.31
8: $z_{\text{abs}} > 1.4$	25	1.33	-1.19	0.31	3.6	-4.16 ± 0.36	1.52 ± 0.19	0.048	4.1	-3.09 ± 0.34	1.53 ± 0.17
9: No H_2	43	1.29	-1.00	0.11	3.9	-4.52 ± 0.46	1.83 ± 0.24	0.025	4.2	-3.38 ± 0.42	1.71 ± 0.22
10: No H_2 or 21-cm	35	1.25	-0.99	0.92	3.3	-4.80 ± 0.54	1.97 ± 0.29	0.40	3.5	-3.49 ± 0.48	1.78 ± 0.25
11: H_2 systems	6	2.78	-0.84	15	2.4	-4.06 ± 0.63	1.44 ± 0.29	91	1.7	-3.26 ± 0.75	1.55 ± 0.32
12: 21-cm systems	9	1.38	-1.20	95	1.7	-3.65 ± 0.68	1.37 ± 0.33	12	2.5	-2.74 ± 0.63	1.30 ± 0.31

sample, may somewhat alter its slope. To explore whether this is indeed the case, we make a simple correction to the metallicities in Table 1 according to

$$[M/H]_{\text{corr}} = 0.52 + [M/H] + 0.27 z_{\text{abs}}. \quad (1)$$

The numerical coefficients are the y-intercept and slope from an unweighted least squares fit to $[M/H]$ versus z_{abs} using the fiducial sample. This has the effect of correcting each metallicity by the expected mean value at the absorber’s redshift. The slope and intercept are consistent with those derived from larger samples of DLAs covering similar redshift ranges (e.g. Prochaska et al. 2003a; Kulkarni et al. 2005). Fig. 1(right) shows the redshift-corrected metallicities versus W_r^{12796} and Table 2 gives the redshift-corrected

statistics: the general scatter around the $[M/H]-W_r^{12796}$ correlation clearly decreases upon correction; the table shows that the significance of the $[M/H]-W_r^{12796}$ correlation increases in almost all sub-samples once the metallicities are corrected for redshift evolution.

Visually, the correlation in Fig. 1(left) appears tighter for the lower- W_r^{12796} half of the sample compared to that for the upper half. That is, the variance in $[M/H]$ about the general $[M/H]-W_r^{12796}$ trend appears smaller at low- W_r^{12796} . However, an F-test reveals only marginal evidence for this: a fit of $[M/H]$ versus W_r^{12796} is performed [see equation (2); Section 3.1], the sample is split into two sub-samples at $W_r^{12796} = 1.4 \text{ \AA}$ and the variance in $[M/H]$ about the fit is calculated for each sub-sample. The ratio of the vari-

ances about the fit is 1.83, but this should occur 15 per cent of the time by chance alone given the sizes of the sub-samples. Using the redshift-corrected metallicities [Fig. 1(right)], the ratio of the variances reduces to 1.64, which has an associated probability of 24 per cent. The marginally increased scatter at high $W_r^{\lambda 2796}$ does reduce the significance of the correlation in the high- $W_r^{\lambda 2796}$ sub-sample compared to the low- $W_r^{\lambda 2796}$ sub-sample (see Table 2); one possibility is that Fig. 1, particularly the redshift-corrected version in Fig. 1(right), defines a lower bound ‘envelope’ to the metallicity at a given $W_r^{\lambda 2796}$ instead of a normal correlation. This should of course be combined with an upper bound envelope at high metallicities since arbitrarily high values are unphysical. A larger sample with robust control over metallicity uncertainties would be required to identify these features and to distinguish between a true correlation and a lower bound envelope.

We have also split the sample into two redshift bins about the fiducial sample’s median, $z_{\text{abs}} = 1.4$. Table 2 shows that the $[\text{M}/\text{H}] - W_r^{\lambda 2796}$ correlation is still well-defined in the high- z_{abs} sub-sample but it is somewhat less statistically significant at low- z_{abs} . However, the fits to both sub-samples, as described in Section 3.1, yield consistent results.

Three main objections might be raised to some of the data we use in Table 1: (i) Some of the metallicities are not derived from Zn and so might be susceptible to dust-depletion effects, even though we have made a crude correction to any metallicities derived using the heavily depleted Fe and Cr ions; (ii) Absorbers with low $W_r^{\lambda 2796}$ might contain a significant number of velocity components which are not completely saturated. While $W_r^{\lambda 2796}$ still provides a measure of velocity spread, Δv , in these systems, $W_r^{\lambda 2796}$ will also depend somewhat on the optical depths of the unsaturated components. Therefore, as the MgII velocity components weaken at lower $[\text{M}/\text{H}]$, one might expect a correlation between $[\text{M}/\text{H}]$ and $W_r^{\lambda 2796}$ which has little to do with the correlation found at higher $W_r^{\lambda 2796}$. One might consider that only systems with $W_r^{\lambda 2796} > 0.7 \text{ \AA}$ should be used since the profile is even more likely to be completely saturated; (iii) Finally, the reliability of sub-DLA metallicities is not as well established in the literature as that for DLAs. It is possible that we do not fully understand the ionization corrections required in some cases or, indeed, the magnitude of the systematics involved in deriving $N(\text{H I})$ in sub-DLAs. For example, Voigt profile $N(\text{H I})$ estimates closer to the flat part of the curve of growth naturally have larger random uncertainties and may become increasingly, systematically influenced by weaker Ly- α forest lines. However, Table 2 shows that the $[\text{M}/\text{H}] - W_r^{\lambda 2796}$ correlation is fairly robust against removal of non-Zn metallicities, systems with $W_r^{\lambda 2796} < 0.7 \text{ \AA}$ or sub-DLAs. Removing all three cases together also leaves a $> 3\sigma$ correlation ($> 3.5\sigma$ after correcting the metallicities for redshift evolution).

Note that our sample contains only one system with $[\text{M}/\text{H}] \leq -1.7$. This is partially a selection effect since the Zn II lines become undetectably weak at low metallicities. However, very few DLAs and sub-DLAs are known with lower metallicities at redshifts $0.2 < z_{\text{abs}} < 2.6$ and comparison with other more complete samples (e.g. Kulkarni et al. 2005; Akerman et al. 2005) shows that our sample is fairly representative of the overall DLA metallicity distribution. Finally, we have included 3 systems in Table 1 which are within 5000 km s^{-1} of the emission redshift of the background QSO. These systems do not show any signs of being associated with the QSO central engine and so are included here. Removing them from the sample makes a negligible difference to our results.

3 DISCUSSION

The $[\text{M}/\text{H}] - W_r^{\lambda 2796}$ correlation found in Fig. 1 is a direct demonstration that the metallicity of strong Mg II absorbers is closely related to their kinematics (but not necessarily the kinematics of the host galaxy; see below). Since the Mg II $\lambda 2796$ transition is so strong, most velocity components in absorbers with $W_r^{\lambda 2796} > 0.3 \text{ \AA}$ are saturated and so $W_r^{\lambda 2796}$ measures the total velocity spread among the components, Δv . Equivalently, it is a measure of the number of velocity components across the profile (e.g. Petitjean & Bergeron 1990). Thus, the $[\text{M}/\text{H}] - W_r^{\lambda 2796}$ correlation demonstrates that the mechanism responsible for producing individual Mg II velocity components and for dispersing them over velocity ranges $\Delta v \sim 20\text{--}1000 \text{ km s}^{-1}$ is related to – and possibly also determines – the metallicity of the absorber.

The results in Fig. 1 bear on the apparent discrepancy between the conclusions drawn by Nestor et al. (2003), whose results suggest a $[\text{M}/\text{H}] - W_r^{\lambda 2796}$ correlation, and York et al. (2006) whose analysis suggests an anti-correlation. Our observed $[\text{M}/\text{H}] - W_r^{\lambda 2796}$ correlation supports the former and seems inconsistent with the latter. One possible explanation may be that York et al. assume a constant dust-to-gas ratio as a function of $N(\text{H I})$, i.e. $E(B - V) \propto N(\text{H I})$. They base this assumption on their observation that the Mg II absorbers they study seem to redden the background QSOs with, on average, an SMC-like dust extinction law. Even if this proves to be true for strong Mg II absorbers, this relation has certainly not been demonstrated in DLAs or sub-DLAs. Indeed, from the detection of SMC-like dust-reddening in > 300 SDSS DLAs at $z_{\text{abs}} > 2.2$, Murphy et al. (2007, in preparation) find that the mean $E(B - V) \approx 7 \times 10^{-3}$ appears not to change over the range $20.3 \leq \log[N(\text{H I})/\text{cm}^{-2}] \leq 21.7$. One caveat may be important here: possible magnitude bias. Nestor et al. assumed that $N(\text{H I})$ is not a strong function of $W_r^{\lambda 2796}$ based on the observations of Rao et al. (2006). The data in Table 1 also reveal no apparent trend in $N(\text{H I})$ with $W_r^{\lambda 2796}$. However, Rao et al. selected relatively bright background QSOs which could provide reasonable signal-to-noise ratios in ultraviolet (UV) *Hubble Space Telescope* (HST) spectra. York et al. suggest that dusty absorbers are therefore unlikely to exist in Rao et al.’s sample and that this dust-bias (relative to deeper surveys like SDSS) may invalidate Nestor et al.’s assumption. From this point of view, it may not be surprising that our results agree with the conclusion of Nestor et al. since most, but not all, of the absorbers in our sample occult relatively bright QSOs.

3.1 Comparison with higher redshift DLAs

At higher redshifts ($1.6 < z_{\text{abs}} < 3.0$), Wolfe & Prochaska (1998) tentatively noted a correlation between Δv and metallicity from a sample of 17 DLAs. Péroux et al. (2003) found a similarly tentative $[\text{Zn}/\text{H}] - \Delta v$ correlation from a larger sample of DLAs and sub-DLAs over the redshift range $1.4 < z_{\text{abs}} < 4.5$. However, Ledoux et al. (2006, hereafter L06) very recently found a relatively tight and clear $[\text{M}/\text{H}] - \Delta v$ correlation from a sample of UVES spectra containing 70 DLAs and sub-DLAs over the range $1.7 < z_{\text{abs}} < 4.3$. They defined Δv from different transitions of several low ionization species (O I, Si II, Fe II, Cr II, S II) with moderate optical depths such that the strongest velocity component absorbed between 10 and 60 per cent of the continuum. Since many of the DLAs in the L06 sample are at $z_{\text{abs}} > 2.6$ where the Mg II lines are not observable with optical spectroscopy, a complete comparison between the L06 sample and ours is difficult. Nevertheless, it

is clear that, since W_r^{12796} is a measure of Δv , the $[M/H]-W_r^{12796}$ correlation in Fig. 1 persists at higher redshifts.

L06 fit their $[M/H]-\Delta v$ data using the least squares bisector method of Isobe et al. (1990), finding the best-fit relationship to be $[M/H] = (1.55 \pm 0.12) \log \Delta v [\text{km s}^{-1}] - (4.33 \pm 0.23)$. For comparison, we performed fits using the same bisector technique after converting our W_r^{12796} values to Δv according to the simple relation $\Delta v [\text{km s}^{-1}] \approx 70 [\text{km s}^{-1} \text{ \AA}^{-1}] \times W_r^{12796} [\text{ \AA}]$. The proportionality constant is derived from a fit of W_r^{12796} versus Δv , with the inverse of the variances on W_r^{12796} used as weights, for the 18 absorbers which appear in both our sample and that of L06. The fiducial sample is best-fitted by the relation

$$[M/H] = (1.69 \pm 0.20) \log \Delta v [\text{km s}^{-1}] - (4.29 \pm 0.38), \quad (2)$$

which is consistent with the relation found by L06.

Table 2 shows the intercept A and slope B of the $[M/H]-\Delta v$ relationship for the different sub-samples. In particular, we find no evidence for significant differences in A or B in the low- and high- z_{abs} sub-samples. This is similar to the results of L06 who find the slope and intercept to be statistically consistent in two redshift bins split at $z_{\text{abs}} = 2.43$. We also note that the median W_r^{12796} and $[M/H]$ of our low- z_{abs} sub-sample are marginally higher than at high- z_{abs} : $\langle W_r^{12796} \rangle = 1.56 \text{ \AA}$ and $\langle [M/H] \rangle = -0.82$ for the former compared with $\langle W_r^{12796} \rangle = 1.33 \text{ \AA}$ and $\langle [M/H] \rangle = -1.19$ for the latter. Again, L06 find similar trends.

3.2 Mass–metallicity correlation or anti-correlation?

The $[M/H]-W_r^{12796}$ (or $[M/H]-\Delta v$) correlation in DLAs and sub-DLAs provides an important link between the kinematics of the absorber and the metal-enrichment history of the absorber. However, one would like to go a step further and link the metallicity with the mass of the halo in which the absorber resides. This step is potentially confusing. For example, many authors have, in the past, tacitly assumed that the absorption-line kinematics are a reliable tracer of the host-galaxy kinematics. That is, Δv is assumed to positively correlate with the circular velocity of the host-galaxy. By presuming this detail of the absorber–galaxy connection – which should instead be observationally determined – one would conclude that W_r^{12796} (and Δv) is correlated with the galaxy mass. L06 make this latter assumption and use it to constrain the implied mass–metallicity relationship. Indeed, they find this to be consistent with the luminosity–metallicity relationship derived from local galaxies.

However, the assumption that galaxy or halo mass is correlated with W_r^{12796} is challenged by new observations. Bouché et al. (2006, hereafter B06) identified 1806 Mg II systems with $W_r^{12796} \geq 0.3 \text{ \AA}$ and ~ 250000 luminous red galaxies (LRGs) within projected co-moving distances of $13h^{-1}$ Mpc of the absorbers. The ratio of the absorber–LRG cross-correlation to the LRG–LRG auto-correlation provides a measure of the bias-ratio between absorbers and LRGs. In hierarchical structure formation scenarios the bias scales with halo mass, so the clustering of LRGs around the Mg II absorbers provides a measure of the absorber halo mass. With this approach, B06 found that halo mass and W_r^{12796} are *anti-correlated*. They also found that by combining the previously observed luminosity- and W_r^{12796} -dependence of the absorber cross-section, or by combining the cross-section’s luminosity-dependence with the observed incidence probability of strong Mg II absorbers, $d^2N/dz_{\text{abs}}dW_r^{12796}$, one finds that luminosity (or mass) and W_r^{12796} should be anti-correlated. Prochter et al. (2006) reached a similar conclusion by

interpreting the observed redshift evolution of the number density of strong Mg II systems with simple cross-section arguments.

Of course, the main difference between the B06 absorber sample and the one studied here is that B06 used strong Mg II absorbers while we study DLAs and strong sub-DLAs. It is possible that a mass– W_r^{12796} correlation does exist for DLAs if the sharp drop in halo-mass observed by B06 for Mg II systems with $W_r^{12796} > 1.0 \text{ \AA}$ were dominated by systems with neutral hydrogen column densities below the lower limit imposed here, i.e. $N(\text{H I}) = 3 \times 10^{19} \text{ cm}^{-2}$. However, this seems very unlikely given that the fraction of strong Mg II systems which are DLAs [i.e. have $N(\text{H I}) = 2 \times 10^{20} \text{ cm}^{-2}$] increases from ~ 15 to ~ 65 per cent over the range $W_r^{12796} = 0.6\text{--}3.3 \text{ \AA}$ (Rao et al. 2006). It is therefore important to confirm or refute the B06 results, which derive from SDSS Data Release 3. Bouché et al. (2007, in preparation) will present an analysis based on a significantly increased sample of absorbers from Data Release 5.

3.3 Are strong Mg II absorbers caused by outflows?

B06 interpret their observed mass– W_r^{12796} anti-correlation as evidence that outflows become the dominant mechanism for producing Mg II absorbers as W_r^{12796} increases beyond $\sim 1.0 \text{ \AA}$. They reason that outflows are more easily ejected from lower mass star-forming galaxies and so, when viewed along a random QSO sightline, are more likely to produce more Mg II velocity components over a larger velocity range. In this outflow picture, W_r^{12796} and the number of Mg II velocity components may be inversely related to the mass and could depend more strongly on the recent star-formation history of the host-galaxy. L06 mention that some fraction of DLAs could be caused by outflows, but they again attribute the outflow velocity spread to be directly related to the depth of the host galaxy’s potential well.

An initial objection to the outflow model for DLAs and strong Mg II systems might be that such hot, highly ionized material may not produce velocity components of cold gas which can be traced with low-ionization species such as Mg II. However, the outflows from local starburst galaxies are well-known to contain clouds of cold gas and dust (Lehnert & Heckman 1996; Martin 1999; Heckman et al. 2000; Rupke et al. 2005; Martin 2006). Dense, molecular gas is also known to be entrained in smaller scale outflows (e.g. Nakai et al. 1987) and even the ionization cones of nearby active galactic nuclei which show starburst activity (e.g. Irwin & Sofue 1992; Curran et al. 1999). Moreover, Norman et al. (1996) identified Mg II absorption in spectra of two QSO sight-lines with impact parameters $25 h^{-1}$ kpc and $55 h^{-1}$ kpc near the galaxy NGC 520, a local starburst with super-winds, a disturbed morphology and filamentary H α emission along its minor axis. Thus, it seems clear that outflows from star-forming galaxies do contain cold gas.

If indeed many high- W_r^{12796} Mg II absorbers are caused by outflows and these outflows do indeed entrain cold clouds (or cold gas clumps cool out of the hotter outflow medium), do we observe tracers of the cold, dusty gas, such as molecular hydrogen? H₂ is identified via UV absorption in the Lyman and Werner bands and is known to arise in very cold, dusty velocity components (e.g. Ledoux et al. 2003). It is therefore notable that 3 of the 5 highest- W_r^{12796} systems in Fig. 1 are known to contain H₂. Indeed, the two highest- W_r^{12796} systems, those towards Q0013-0029 and Q0551-366, both contain H₂ (Ledoux et al. 2002; Petitjean et al. 2002) and have W_r^{12796} values at the extreme of the W_r^{12796} distribution obtained from large SDSS Mg II surveys (e.g. Nestor et al. 2003; Prochter et al. 2006). The median W_r^{12796} for the H₂ absorbers in

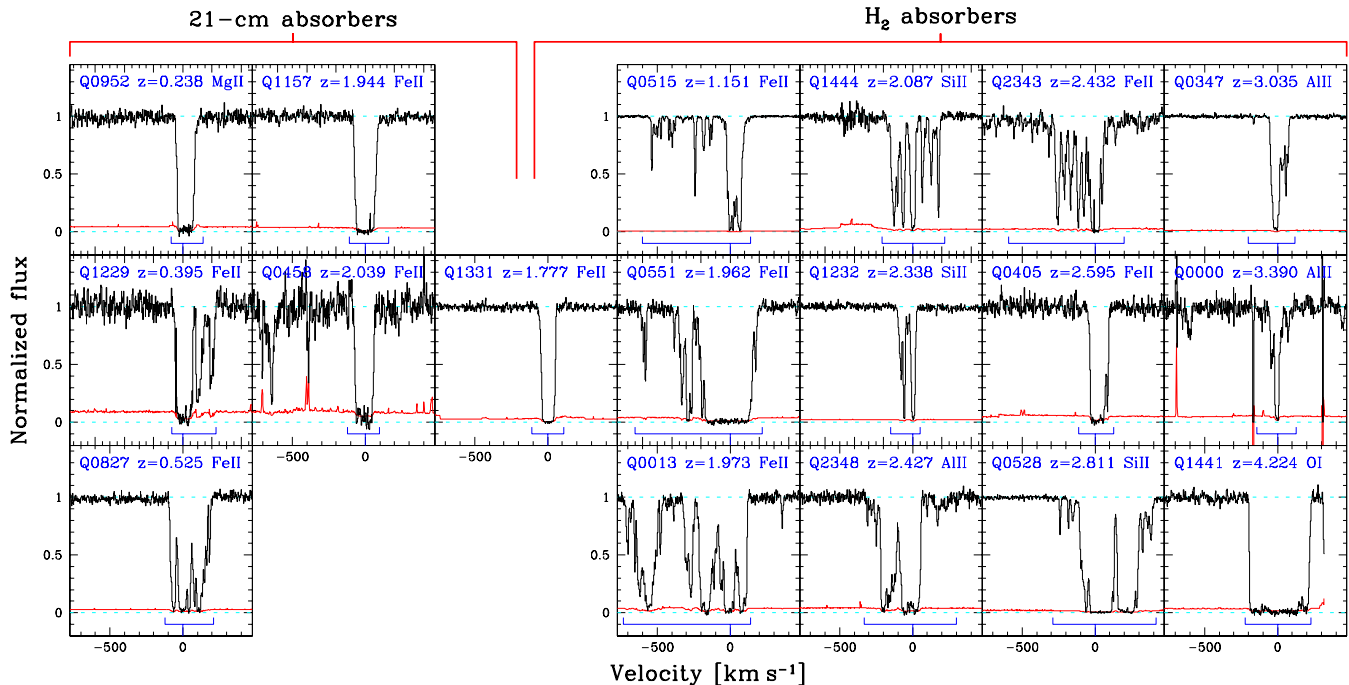


Figure 2. Montage of the velocity structures of strong transitions in the 13 known H₂-bearing DLAs/sub-DLAs in the literature (6 are in our sample) and the 21-cm absorbers in our sample. The transition used to illustrate the extent and distribution of absorption components is marked on each panel. In most cases the Fe II λ 2382 line is used. Fe II λ 2600 is used for the absorber towards Q 0458–020. When Fe II λ 2382 was not available (particularly at high- z_{abs}), O I λ 1302, Si II λ 1526, Al II λ 1670 or Mg II λ 2796 is used. All systems are shown on a common velocity scale registered to the redshift of the strongest H₂ or 21-cm component in each system. The black histogram is the data normalized by a local continuum fit while the grey/red line near zero flux shows the normalized 1σ error array. The approximate extent of the transitions is marked by the bracket below the zero level. Note the similarity in the profiles for many of the H₂-bearing systems. These broad and complex structures may be characteristic of outflows. The 21-cm profiles generally do not show such outflow signatures, but the sample is too small for strong conclusions to be made.

our sample is 2.8 \AA compared with 1.4 \AA for the sample as a whole (Table 2). Even with only six H₂ systems, a Kolmogorov-Smirnov test gives a probability of just 9 per cent that the equivalent widths of the H₂ absorbers are drawn from the same parent population as the rest of the sample.

In Fig. 2 we compare the velocity structures of all the 13 known H₂-bearing DLAs and sub-DLAs. It is striking how similar the velocity structures are for the systems towards Q 0515–4414, Q 0551–366 and Q 0013–0029: each is spread over $\Delta v \geq 700 \text{ km s}^{-1}$ and comprises at least three groups of stronger velocity components separated by few (if any) weaker components. The systems towards Q 1444+014 and Q 2343+125 have very similar profiles and these are not dissimilar to the above three. Also, the systems towards Q 2348–011 and Q 0528–250 both have two broad, saturated regions separated by a narrow region of low optical depth. Such structures and symmetries have been discussed by Bond et al. (2001) and Ellison et al. (2003) as being the characteristic signs of absorption in galactic outflows. It is also conceivable that these profiles are produced in galaxy mergers (but see discussion in Bond et al. 2001).

Although no strong conclusions can be reached due to the sample size, Fig. 2 nevertheless suggests that approximately half of the known H₂-bearing systems may arise in outflows. If indeed cold gas and dust is entrained in outflows and the gas is well-shielded then H₂ should form on the surface of dust-grains. Even if this happens in very few clouds, the large number of clouds across these profiles significantly increases the probability of observing one or more H₂-bearing clouds towards any given background QSO.

Hence, even if these outflow-like absorption profiles are themselves rare, H₂ may be found within them in a large fraction of cases.

Fig. 2 also shows the velocity structures of the 21-cm absorbers in our sample for which UVES spectra were available. These velocity structures are typical of those in the general population, seemingly consistent with the fact that the 21-cm absorbers are generally indistinct from most other systems in the $[M/H]-W_r^{12796}$ plane (Fig. 1). Like H₂ absorption, 21-cm absorption should arise in cold clouds, but there is no evidence in Fig. 2 to suggest that 21-cm absorbers also arise in the complicated and broad outflow-like profiles like the H₂ systems. However, the 21-cm sample is very small and is dominated by low- z_{abs} systems; outflows are likely to be less common below $z_{\text{abs}} \sim 1$ due to the general decline in the global star-formation rate density (see, e.g., Bond et al. 2001).

L06 note that, under the assumption of a mass-metallicity relationship, the absorbers with the highest equivalent widths and metallicities will be most easily detected in direct imaging observations. This prediction is also natural in the outflow picture where W_r^{12796} and the number of Mg II velocity components are related to both the mass and the recent star-formation history of the absorber host-galaxy. While one expects the highest W_r^{12796} and highest $[M/H]$ systems to be hosted by lower mass galaxies, they should be actively star-forming and show strong H α emission. If indeed H₂-bearing systems more often probe star-forming galaxies with outflows, they may be more reliable tracers of the cosmological evolution of metallicity than other DLAs, many of which might not be closely linked to star-formation sites/processes in high- z galaxies. We have already advanced this possibility in Curran et al. (2004) and Murphy et al. (2004) based on a comparison of H₂ ab-

sorber metallicities with those of the general DLA population. The H₂ absorbers showed a faster, more well-defined increase in [M/H] with decreasing redshift, although the sample was quite small. A much larger sample of H₂-bearing systems is required to compute the $N(\text{H I})$ -weighted metallicity evolution in a way comparable with general DLA samples.

4 CONCLUSIONS

For 49 DLAs and sub-DLAs with published metallicities we have measured or gathered from the literature their Mg II rest-frame equivalent widths to search for an empirical relationship between the kinematic spread, Δv , in the absorbing metal-line velocity components and the total absorber metallicity. The vast majority of DLAs and strong sub-DLAs have $W_r^{12796} > 0.3 \text{ \AA}$ which means that most Mg II velocity components across the absorption profile are saturated. Thus, W_r^{12796} provides a simple measure of Δv which can be derived even from relatively low-resolution QSO spectra.

We find a correlation between [M/H] and W_r^{12796} at the significance level of 4.2σ [Fig. 1(left)] which increases to 4.7σ when the [M/H] values are corrected for mild cosmological evolution over the sample's redshift range of $0.2 < z_{\text{abs}} < 2.6$ [Fig. 1(right)]. Even for our most conservative sub-sample, where we include only 26 DLAs (no sub-DLAs) with Zn-metallicities and $W_r^{12796} > 0.7 \text{ \AA}$, we still find a correlation at $> 3 \sigma$ ($> 3.5 \sigma$ after redshift-correction of [M/H]). After converting the W_r^{12796} values to Δv , the slope of our [M/H]– $\log \Delta v$ relationship is consistent with that reported recently by Ledoux et al. (2006) for generally higher- z_{abs} DLAs and sub-DLAs, suggesting that the [M/H]– W_r^{12796} correlation persists up to $z_{\text{abs}} = 4.7$. Although we find a lower statistical significance for the correlation below $z_{\text{abs}} = 1.4$, the fitted slope and intercept of the [M/H]– $\log \Delta v$ data is similar for the $z_{\text{abs}} < 1.4$ and $z_{\text{abs}} > 1.4$ sub-samples. Finally, we find marginal ($\sim 1.4 \sigma$) evidence for increased variance in metallicity above $W_r^{12796} = 1.4 \text{ \AA}$. However, the evidence weakens once the [M/H] values are corrected for evolution; other non-intrinsic sources of metallicity scatter may need to be addressed before such an effect can be verified.

If one assumes that the metal-line absorption kinematics trace the host-galaxy kinematics – that Δv is proportional to the host-galaxy circular velocity – then it is natural to translate the observed [M/H]– W_r^{12796} correlation into a correlation between [M/H] and galaxy mass. Indeed, Ledoux et al. (2006) make this assumption and find that the resulting [M/H]–mass correlation is consistent with the [M/H]–luminosity relationship derived from local galaxies. However, by studying the clustering of galaxies around strong Mg II absorbers in the SDSS, Bouché et al. (2006) find that mass is anti-correlated with W_r^{12796} . This result, together with the [M/H]– W_r^{12796} relationship observed here, implies that the absorber metallicity is anti-correlated with halo or galaxy mass. It is therefore important to confirm or refute the results of Bouché et al. and to address the assumption of Ledoux et al. (2006) with observations.

Finally, we note that about half of the known H₂ absorbers have very broad velocity structures which show distinct distributions of velocity components (Fig. 2). The patterns, groups and symmetries evident in these cases are consistent with an outflow origin for the bulk of the components. Since outflows can entrain cold, dusty gas and since they should provide a large number of velocity components, the probability of finding one or more H₂-bearing components in any given outflow-driven absorber might be quite high, even though H₂-bearing components are themselves quite rare. This suggests the targeting of high- W_r^{12796} absorbers to

identify more H₂-bearing systems. Given the [M/H]– W_r^{12796} correlation we observe, this may be similar to the metallicity-selection approach of Petitjean et al. (2006). However, it has the advantage that one can determine W_r^{12796} with only moderate-resolution spectra – or infer it from the equivalent width of bluer transitions when $z_{\text{abs}} \gtrsim 2.5$ – which need not be blue- or UV-sensitive (e.g. SDSS spectra). One can then follow-up the highest W_r^{12796} systems with high-resolution, UV- or blue-sensitive spectra to search for H₂ absorption.

ACKNOWLEDGMENTS

We thank N. Bouché for many discussions and critical comments which significantly improved the paper and S. Ellison for providing her W_r^{12796} measurements. We also thank H.-W. Chen for comments on an early draft. MTM thanks PPARC for an Advanced Fellowship. Some of this research was based on observations made with ESO Telescopes at the Paranal Observatories under programme IDs listed in Table 1. This research has made use of the NASA/IPAC Extragalactic Database (NED) which is operated by the Jet Propulsion Laboratory, California Institute of Technology, under contract with the National Aeronautics and Space Administration. This research has also made use of NASA's Astrophysics Data System Bibliographic Services.

REFERENCES

- Akerman C. J., Ellison S. L., Pettini M., Steidel C. C., 2005, *A&A*, 440, 499
- Aldcroft T. L., Bechtold J., Elvis M., 1994, *ApJS*, 93, 1
- Bergeron J., Boissé P., 1991, *A&A*, 243, 344
- Bergeron J., Cristiani S., Shaver P. A., 1992, *A&A*, 257, 417
- Boisse P., Le Brun V., Bergeron J., Deharveng J., 1998, *A&A*, 333, 841
- Bond N. A., Churchill C. W., Charlton J. C., Vogt S. S., 2001, *ApJ*, 562, 641
- Bouché N., Murphy M. T., Péroux C., Csabai I., Wild V., 2006, *MNRAS*, 371, 495
- Boulade O., Kunth D., Tytler D., Vigroux L., 1987, in Bergeron J., Kunth D., Rocca-Volmerange B., Tran Thanh van J., eds, *High Redshift and Primeval Galaxies*. Gif-sur-Yvette: Editions Frontières, France, p. 349
- Centurión M., Molaro P., Vladilo G., Péroux C., Levshakov S. A., D'Odorico V., 2003, *A&A*, 403, 55
- Chen H.-W., Lanzetta K. M., 2003, *ApJ*, 597, 706
- Christensen L., Schulte-Ladbeck R. E., Sánchez S. F., Becker T., Jahnke K., Kelz A., Roth M. M., Wisotzki L., 2005, *A&A*, 429, 477
- Churchill C. W., Mellon R. R., Charlton J. C., Jannuzi B. T., Kirhakos S., Steidel C. C., Schneider D. P., 2000, *ApJ*, 543, 577
- Churchill C. W., Mellon R. R., Charlton J. C., Vogt S. S., 2003, *ApJ*, 593, 203
- Curran S. J., Rydbeck G., Johansson L. E. B., Booth R. S., 1999, *A&A*, 344, 767
- Curran S. J., Webb J. K., Murphy M. T., Carswell R. F., 2004, *MNRAS*, 351, L24
- de la Varga A., Reimers D., Tytler D., Barlow T., Burles S., 2000, *A&A*, 363, 69
- Dessauges-Zavadsky M., Calura F., Prochaska J. X., D'Odorico S., Matteucci F., 2004, *A&A*, 416, 79
- Dessauges-Zavadsky M., Péroux C., Kim T.-S., D'Odorico S., McMahon R. G., 2003, *MNRAS*, 345, 447
- Dessauges-Zavadsky M., Prochaska J. X., D'Odorico S., Calura F., Matteucci F., 2006, *A&A*, 445, 93
- Djorgovski S. G., Pahre M. A., Bechtold J., Elston R., 1996, *Nat*, 382, 234
- Drinkwater M. J., Webster R. L., Thomas P. A., 1993, *AJ*, 106, 848
- Ellison S. L., 2006, *MNRAS*, 368, 335

- Ellison S. L., Mallén-Ornelas G., Sawicki M., 2003, *ApJ*, 589, 709
- Heckman T. M., Lehnert M. D., Strickland D. K., Armus L., 2000, *ApJS*, 129, 493
- Irwin J. A., Sofue Y., 1992, *ApJ*, 396, L75
- Isobe T., Feigelson E. D., Akritas M. G., Babu G. J., 1990, *ApJ*, 364, 104
- Junkkarinen V. T., Cohen R. D., Beaver E. A., Burbidge E. M., Lyons R. W., Madejski G., 2004, *ApJ*, 614, 658
- Khare P., Kulkarni V. P., Lauroesch J. T., York D. G., Crotts A. P. S., Nakamura O., 2004, *ApJ*, 616, 86
- Kulkarni V. P., Fall S. M., Lauroesch J. T., York D. G., Welty D. E., Khare P., Truran J. W., 2005, *ApJ*, 618, 68
- Lanzetta K. M., Bowen D., 1990, *ApJ*, 357, 321
- Lanzetta K. M., Bowen D. V., 1992, *ApJ*, 391, 48
- Lanzetta K. M., McMahon R. G., Wolfe A. M., Turnshek D. A., Hazard C., Lu L., 1991, *ApJS*, 77, 1
- Le Brun V., Bergeron J., Boisse P., Deharveng J. M., 1997, *A&A*, 321, 733
- Ledoux C., Bergeron J., Petitjean P., 2002, *A&A*, 385, 802
- Ledoux C., Petitjean P., Fynbo J. P. U., Møller P., Srianand R., 2006, *A&A*, 457, 71 (L06)
- Ledoux C., Petitjean P., Srianand R., 2003, *MNRAS*, 346, 209
- Ledoux C., Srianand R., Petitjean P., 2002, *A&A*, 392, 781
- Lehnert M. D., Heckman T. M., 1996, *ApJ*, 462, 651
- Lodders K., 2003, *ApJ*, 591, 1220
- Lopez S., Ellison S. L., 2003, *A&A*, 403, 573
- Lopez S., Reimers D., Gregg M. D., Wisotzki L., Wucknitz O., Guzman A., 2005, *ApJ*, 626, 767
- Lopez S., Reimers D., Rauch M., Sargent W. L. W., Smette A., 1999, *ApJ*, 513, 598
- Martin C. L., 1999, *ApJ*, 513, 156
- Martin C. L., 2006, *ApJ*, 647, 222
- Meyer D. M., Lanzetta K. M., Wolfe A. M., 1995, *ApJ*, 451, L13
- Meyer D. M., York D. G., 1992, *ApJ*, 399, L121
- Møller P., Warren S. J., 1993, *A&A*, 270, 43
- Murphy M. T., Curran S. J., Webb J. K., 2004, in Duc P.-A., Braine J., Brinks E., eds, *IAU Symp. Ser. Vol. 217, Recycling intergalactic and interstellar matter*. Astron. Soc. Pac., San Francisco, CA, U.S.A, p. 252
- Nakai N., Hayashi M., Handa T., Sofue Y., Hasegawa T., Sasaki M., 1987, *Publ. Astron. Soc. Japan*, 39, 685
- Nestor D. B., Rao S. M., Turnshek D. A., Vanden Berk D., 2003, *ApJ*, 595, L5
- Norman C. A., Bowen D. V., Heckman T., Blades C., Danly L., 1996, *ApJ*, 472, 73
- Péroux C., Dessauges-Zavadsky M., D'Odorico S., Kim T., McMahon R. G., 2003, *MNRAS*, 345, 480
- Péroux C., Deharveng J.-M., Le Brun V., Cristiani S., 2004, *MNRAS*, 352, 1291
- Péroux C., Kulkarni V. P., Meiring J., Ferlet R., Khare P., Lauroesch J. T., Vladilo G., York D. G., 2006, *A&A*, 450, 53
- Petitjean P., Bergeron J., 1990, *A&A*, 231, 309
- Petitjean P., Ledoux C., Noterdaeme P., Srianand R., 2006, *A&A*, 456, L9
- Petitjean P., Srianand R., Ledoux C., 2002, *MNRAS*, 332, 383
- Pettini M., Ellison S. L., Steidel C. C., Bowen D. V., 1999, *ApJ*, 510, 576
- Pettini M., Ellison S. L., Steidel C. C., Shapley A. E., Bowen D. V., 2000, *ApJ*, 532, 65
- Pettini M., King D. L., Smith L. J., Hunstead R. W., 1997, *ApJ*, 478, 536
- Prochaska J. X., Gawiser E., Wolfe A. M., 2001, *ApJ*, 552, 99
- Prochaska J. X., Gawiser E., Wolfe A. M., Castro S., Djorgovski S. G., 2003a, *ApJ*, 595, L9
- Prochaska J. X., Gawiser E., Wolfe A. M., Cooke J., Gelino D., 2003b, *ApJS*, 147, 227
- Prochaska J. X., O'Meara J. M., Herbert-Fort S., Burles S., Prochter G. E., Bernstein R. A., 2006, *ApJ*, 648, L97
- Prochaska J. X., Wolfe A. M., 1999, *ApJS*, 121, 369
- Prochter G. E., Prochaska J. X., Burles S. M., 2006, *ApJ*, 639, 766
- Rao S. M., Nestor D. B., Turnshek D. A., Lane W. M., Monier E. M., Bergeron J., 2003, *ApJ*, 595, 94
- Rao S. M., Turnshek D. A., 2000, *ApJS*, 130, 1
- Rao S. M., Turnshek D. A., Briggs F. H., 1995, *ApJ*, 449, 488
- Rao S. M., Turnshek D. A., Nestor D. B., 2006, *ApJ*, 636, 610
- Rupke D. S., Veilleux S., Sanders D. B., 2005, *ApJS*, 160, 115
- Ryabinkov A. I., Kaminker A. D., Varshalovich D. A., 2003, *A&A*, 412, 707
- Ryan-Weber E. V., Webster R. L., Staveley-Smith L., 2003, *MNRAS*, 343, 1195
- Spinrad H., McKee C. F., 1979, *ApJ*, 232, 54
- Steidel C. C., Dickinson M., Persson S. E., 1994, *ApJ*, 437, L75
- Steidel C. C., Sargent W. L. W., 1992, *ApJS*, 80, 1
- Weatherley S. J., Warren S. J., Møller P., Fall S. M., Fynbo J. U., Croom S. M., 2005, *MNRAS*, 358, 985
- Wolfe A. M., Briggs F. H., Turnshek D. A., Davis M. M., Smith H. E., Cohen R. D., 1985, *ApJ*, 294, L67
- Wolfe A. M., Prochaska J. X., 1998, *ApJ*, 494, L15
- Wolfe A. M., Turnshek D. A., Smith H. E., Cohen R. D., 1986, *ApJS*, 61, 249
- York D. G. et al., 2006, *MNRAS*, 367, 945

This paper has been typeset from a $\text{\TeX}/\text{\LaTeX}$ file prepared by the author.